Soil infiltration characteristics and pore distribution under freezing-thawing conditions

Ruiqi Jiang[1,2,3,★], Tianxiao Li[1,2,3,★], Dong Liu[1,2,3,*], Qiang Fu [1,2,3,*], Renjie Hou [1,2,3],

Qinglin Li [1], Song Cui [1,2,3], Mo Li [1,2,3]

[1] School of Water Conservancy & Civil Engineering, Northeast Agricultural University, Harbin 150030, China

[2] Key Laboratory of Effective Utilization of Agricultural Water Resources of Ministry of Agriculture, Northeast Agricultural University, Harbin, Heilongjiang 150030, China

[3] Heilongjiang Provincial Key Laboratory of Water Resources and Water Conservancy Engineering in Cold Region, Northeast Agricultural University, Harbin, Heilongjiang 150030, China

* Dong Liu and Qiang Fu are corresponding authors.

★ These authors contributed equally to this work.

*Corresponding author at: School of Water Conservancy and Civil Engineering, Northeast Agricultural University, Harbin, Heilongjiang 150030, China

Correspondence to: liudong9599@yeah.net (Dong Liu). fuqiang0629@126.com (Qiang Fu)

Abstract. Frozen soil infiltration widely occurs in hydrological processes such as seasonal soil freezing and thawing, snowmelt infiltration, and runoff. Accurate measurement and simulation of parameters related to frozen soil infiltration processes are highly important for agricultural water management, environmental issues and engineering problems in cold regions. Temperature changes cause soil pore size distribution variations and consequently dynamic infiltration capacity changes during different freeze-thaw periods. To better understand these complex processes and to reveal the freeze-thaw action effects on soil pore distribution and infiltration capacity, black soils, meadow soils and chernozem were selected as test subjects, these soil types account for the largest arable land area in Heilongjiang Province, China. Laboratory tests of

soils at different temperatures were conducted using a tension infiltrometer and ethylene glycol aqueous solution. The stable infiltration rate and hydraulic conductivity were measured, and the soil pore distribution was calculated. The results indicated that for the different soil types, macropores, which constituted approximately 0.1% to 0.2% of the soil volume under unfrozen conditions, contributed approximately 50% of the saturated flow, and after soil freezing, the soil macropore proportion decreased to 0.05% to 0.1%, while the saturated flow proportion decreased to approximately 30%. Soil moisture froze into ice crystals inside relatively large pores, resulting in numerous smaller-sized pores, which reduced the number of macropores but increased the number of smaller-sized mesopores, so that the frozen soil infiltration capacity was no longer solely dependent on the macropores. After the ice crystals had melted, more pores were formed within the soil, enhancing the soil permeability.

Key words: Freezing-thawing soil; Hydraulic conductivity; Pore distribution; Macropores; Infiltration characteristics

1 Introduction

Over the last few decades, the temperature changes caused by global warming have altered the freezing state of near-surface soils, and in China, changes in characteristic values such as the extent of the mean annual area of the seasonal soil freeze/thaw state and maximum freezing depth, indicate the degradation of frozen soil, especially at high latitudes (Wang et al., 2019;Peng et al., 2016). Under the effect of temperature, most frozen regions experience seasonal freezing and thawing of soil, accompanied by coupled soil water and heat movement as well as frost heave processes, thus making the soil structure and function more variable (Oztas and Fayetorbay, 2003;Fu et al., 2019;Gao et al., 2018). Parameters such as the soil infiltration rate and hydraulic conductivity are key factors in the study of soil water movement, groundwater recharge, and solute and contaminant transport simulation (Angulo-Jaramillo et al., 2000). In regard to unfrozen soils,

46   temperature has been shown to change the soil structure and kinematic viscosity of soil water, thereby

47   affecting the unsaturated hydraulic conductivity of soils (Gao and Shao, 2015). In terms of frozen soils, the

48   water infiltration characteristics and pore size distribution are highly variable and difficult to observe

49   (Watanabe et al., 2013); moreover, the water movement in freezing-thawing soils is complicated by the

50   migration of water and heat and the associated water phase change (Jarvis et al., 2016;Hayashi, 2013). The

51   accurate measurement of water movement parameters and soil pore distribution under freeze-thaw

52   conditions is a necessary prerequisite for the quantitative description of the water movement in frozen soil,

53   and the mechanism and degree of influence of the temperature on the infiltration rate, hydraulic conductivity,

54   porosity and other parameters in the different stages of freeze-thaw periods require further research.

55   Currently, quantitative studies of the infiltration process in freezing-thawing soils can be mainly divided into

56   experimental and model studies. Field experiments have been performed less often because under natural

57   conditions, infiltration water exhibits a preferential flow into the deep soil, and the alternating freeze-thaw

58   effect forms ice crystals to block the flow path through large pores, subsequently limiting water infiltration

59   (Daniel et al., 1997), while the melting effect of the infiltration water on ice makes it difficult to reach a

60   steady infiltration state. Therefore, the current relevant achievements are mainly focused on the infiltration

61   process of snowmelt water (Hayashi et al., 2003) and the influence of preferential flow (Mohammed et al.,

62   2019). Controlled laboratory experiments provide new opportunities for the simulation of frozen soil

63   infiltration processes and the measurement of infiltration parameters. Williams and Burt (1974) conducted

64   early direct measurements in the laboratory, resolved the water freezing problem by adding lactose and

65   applied dialysis membranes on both sides of soil columns, and they determined the water conductivity of

66   saturated specimens in the horizontal direction (Burt and Williams, 1976). Andersland et al. (1996) measured

67   the hydraulic conductivity of frozen granular soils at different saturations using a conventional drop

68   permeameter with decane as the permeant and concluded that the hydraulic conductivity was the same as

69   that of unfrozen soils with water as the infiltration solution. McCauley et al. (2002) determined and compared

70   the differences in hydraulic conductivity, permeability and infiltration rate between frozen and unfrozen soils

71   using diesel mixtures as permeants, and their results indicated that the ice content determines whether soil is

72   sufficiently impermeable. Zhao et al. (2013) quantified the unsaturated hydraulic conductivity of frozen soil

73   using antifreeze instead of water, and adopted a multistage outflow method under controlled pressures in

74   combination with the concept of the pore impedance coefficient (Jame and Norum, 1980). However, most

75   of these studies did not consider the differences in kinematic viscosity and surface tension between soil water

76   and other solutions, which often results in an overestimation of hydraulic conductivity, and homemade

77   devices in the laboratory are often inconvenient for generalization in the field. Due to the dynamic changes

78   in the temperature and moisture phase, direct measurement is difficult, and hydraulic conductivity empirical

79   equations and models of frozen soil have been developed. First, the frozen soil hydraulic conductivity was

80   simply considered to follow a power exponential relationship with the temperature (Nixon, 1991;Smith,

81   1985), while others considered the hydraulic conductivity of frozen soil to be equal to that of unfrozen soil

82   at the same water content and assumed that the hydraulic conductivity of frozen soil was a function of the

83   moisture content of unfrozen soil (Lundin, 1990;Flerchinger and Saxton, 1989;Harlan, 1973). On the basis

84   of Campbell's model (Campbell, 1985), Tarnawski and Wagner (1996) proposed a frozen soil hydraulic

85   conductivity model based on the soil particle size distribution and porosity. Watanabe and Wake (2008)

86   viewed soil pores as cylindrical capillaries and suggested that ice formation occurs at the center of these

87   capillaries and established a model to describe the movement of thin film water and capillary water in frozen

88   soil based on the theory of capillaries and surface absorption (Watanabe and Flury, 2008). The similarity

89   between freezing and soil moisture profiles has been demonstrated (Spaans and Baker, 1996;Spaans, 1994),

90   and subsequently, soil freezing characteristic curves have been applied to estimate the unsaturated hydraulic

91   conductivity of frozen soils (Azmatch et al., 2012), which has been combined with field tests and inversion

92   models to achieve a high accuracy (Cheng et al., 2019).

93   Understanding the distribution characteristics of the soil pore system is essential for the evaluation of the

94   water and heat movement processes in soil. Soil macroporosity has been shown to impose a major impact

95   on water cycle processes such as infiltration, nutrient movement and surface runoff. (Demand et al.,

96   2019;Jarvis, 2007). Macroporosity is widespread in a variety of soils and produces preferential flow in both

97   frozen and unfrozen soils (Mohammed et al., 2018;Beven and Germann, 2013), and the pre-freeze moisture

98   conditions affect the amount and state of ice in the macropores of frozen soils, resulting in notable variability

99   in the infiltration capacity of thawed soils (Hayashi et al., 2003;Granger et al., 1984). Field experiments on

100   frozen soil have also demonstrated that macropores accelerate the infiltration rate (Stähli et al., 2004;Kamp

101   et al., 2003), the number and size of macropores affect the freezing and infiltration capacity of soil layers to

102   different extents, and low temperatures cause infiltration water to refreeze inside macropores (Watanabe and

103   Kugisaki, 2017;Stadler et al., 2000). Research on frozen soil macroporosity has largely focused on the

104   qualitative analysis of its impact on the soil structure and infiltration capacity, and with the development of

105   experimental techniques, certain new methods and techniques, such as computed tomography (CT) and X-

106   ray scanning, have been applied to measure the number and distribution of macropores (Taina et al.,

107   2013;Bodhinayake et al., 2004;Grevers et al., 1989), but the lack of sampling techniques targeting frozen

108   soil still restricts related research.

109   Many limitations and deficiencies remain in the direct measurement of frozen soil infiltration characteristics

110   and pore distribution, and the relevant models also require a large amount of measured data to meet the

111   accuracy and applicability requirements. In this paper, the stable infiltration rate and hydraulic conductivity

of three types of soils at different temperatures were measured by precise control of the soil and ambient temperatures, and the macropore and mesopore size distribution was calculated by using a tension infiltrometer and a glycol aqueous solution as the infiltration medium. The conclusions provide a basis and reference for the numerical simulation of the coupled water-heat migration process of freezing-thawing soil and related parameterization studies.

2 Materials and methods

2.1 Test plan

Referring to arable land area data of various regions of Heilongjiang Province, the three types of soils that dominate the cultivated land area in this province are black soils, meadow soils and chernozem (Bureau, 1992). Harbin, Zhaoyuan and Zhaozhou were selected as typical soil areas for sampling. A 5-cm surface layer of floating soil and leaves was removed, and topsoil samples were collected at depths ranging from 0-20 cm. After natural air drying and artificial crushing, the soil was sieved, and particles larger than 2 mm in diameter were removed. The remainder was used to prepare soil columns. The basic physical and chemical parameters of the test soils, such as the bulk density, organic content and mechanical parameters, are listed in Table 1.

An artificial climate chamber was applied to control the temperature of the soil column and infiltration solution, and four temperature treatments were established with three replications for each treatment: 15°C, unfrozen soil, representing the soil before freezing, which was recorded as 15°C (BF); -5°C, stable freezing; -10°C, stable freezing; and freezing at -10°C followed by thawing at 15°C, representing the soil after melting, which was recorded as 15°C (AM). Each soil column was tested for only one treatment. The freezing and thawing times were both 48 h. When the soil temperature was consistent with the set temperature in the climate chamber, the samples were considered to be completely frozen, and the effect of the number of

freezing and thawing cycles was not considered in this test. According to the basic information of the original

soil, the volumetric moisture content of the sieved soil was set to 30%±2% using deionized water, with a

dry bulk density of 1.2 g/cm^3. To reduce the inhomogeneous distribution of soil moisture, a spray bottle was

used to add water to the sieved and air-dried soil in small but repeated amounts, while the change in soil

moisture was detected using sensors, so that the moisture content of the soil columns was controlled within

the set range and the texture was uniform, as well as making the pre-freeze moisture content relatively

consistent between different soil columns. The soil porosity and pre-freezing soil water content of the

repacked samples are shown in Table 2.

Table 1

Basic physical and chemical properties of three kinds of soils

Soil types	Bulk density (g/cm^3)	Organic content (g/kg)	Electrical conductivity (s/m)	Particle size (sand-silt-clay) (%)	Soil texture
Black soil	1.31	28.32	0.02	12.64-70.82-16.54	
Meadow soil	1.22	16.51	0.01	9.52-73.00-17.48	silt loam
Chernozem	1.15	26.52	0.01	38.99-50.30-10.71	

Table 2

Soil porosity and pre-freezing soil water content of repacked samples

Soil types	Soil porosity (%)	Pre-freeing water content (%)	
		-5°C	-10°C
Black soil	52.76	30.53	29.27
Meadow soil	52.82	29.83	30.70
Chernozem	53.22	30.07	30.93

146   To ensure a homogeneous column, the soil was loaded into a polyvinyl chloride (PVC) cylinder at 5-cm

147   depth intervals, and petroleum jelly was applied to the sides to reduce the sidewall flow (Lewis and Sjöstrom,

148   2010). The PVC cylinder was 26 cm in diameter and 30 cm in height, with a perforated plate at the bottom.

149   To prevent lateral seepage, the barrel occurred 5 cm above the soil surface, and the thickness of the soil layer

150   was 20 cm. A HYDRA-PROBE II sensor (STEVENS Water Monitoring Systems, Inc., Portland, Oregon,

151   USA) was inserted in the middle of the barrel to observe the potential soil temperature and liquid water

152   content change to determine whether ice melting occurred, and the ice content of frozen soil was measured

153   by the drying method. A 5-cm thick layer of sand and gravel was placed below the soil column, and a 5-cm

154   thick layer of black polypropylene insulation cotton was wrapped around the outer layer and the bottom of

155   the soil column. The stable infiltration rate under tension levels of -3, -5, -7, -9, -11, and -13 cm was measured

156   with a tension infiltrometer, and the infiltration time and cumulative infiltration were recorded. The detailed

157   layout of the test apparatus is shown in Fig. 1.

158   The addition of a certain amount of lactose, antifreeze or other substances to water greatly reduces the

159   freezing point of water (Zhao et al., 2013;Williams and Burt, 1974) so that the soil macropores are not

160   quickly filled with ice with decreasing temperature, thereby maintaining better conditions for water flow. To

161   further verify the feasibility of the use of deionized water to prepare an aqueous solution of ethylene glycol

162   at a mass concentration of 40% as the infiltration medium for the frozen soil measurements, the surface

163   tension of the aqueous glycol solution at -5°C and -10°C and its relationship with the temperature were

164   measured with a contact angle measuring instrument (OCA20, DataPhysics Instruments, Germany) and a

165   surface tension measuring instrument (DCAT-21, DataPhysics Instruments, Germany), respectively. As an

166   example, the contact angle measurement process of the black soil at -10°C with the aqueous ethylene glycol

167   solution is shown in Fig. 2, and it is observed that the contact angle decreases to 0° within a few seconds

168   after the liquid droplet is placed on the soil, and the liquid droplet completely dissolves in the frozen soil,

169   which implies that the addition of glycol to water does not alter the wetting ability of the soil particles (Lu

170   and Likos, 2004). For the unfrozen soils of the 15°C (BF) and 15°C (AM) treatments, deionized water was

171   used as the infiltration solution, and for the frozen soils of the -5°C and -10°C treatments, aqueous ethylene

172   glycol solution was used as the infiltration solution. The relevant physicochemical properties of the aqueous

173   ethylene glycol solution and water are compared in Table 3.

174
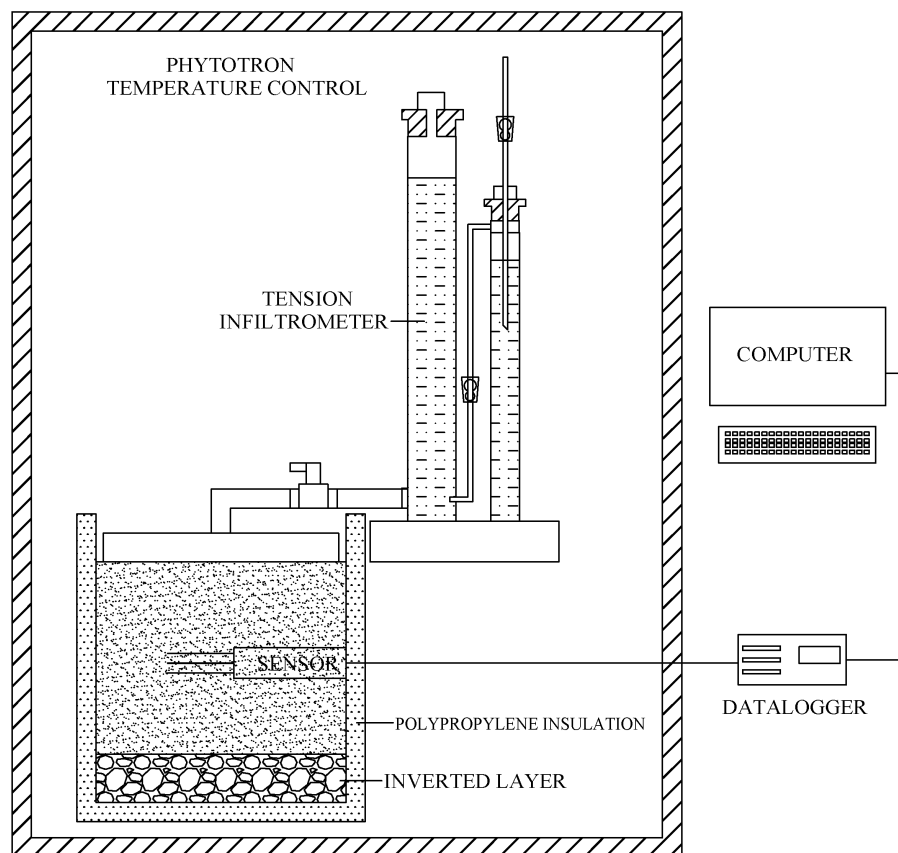
175   **Fig. 1**. Diagram of the test equipment.

176

177   **Fig. 2**. Process of the contact angle measurement between the aqueous ethylene glycol solution and black

178   soil at -10°C.

179 **Table 3**

180 **Comparison of the physicochemical properties of the 40% ethylene glycol aqueous solution and**

181 **water**

Infiltration solution	Temperature (°C)	Density (g/cm^3)	Dynamic viscosity (mPa·s)	Surface tension (mN/m)	Contact angle (°)
Water	15	0.9991	1.14	73.56	0
Ethylene glycol	-5	1.0683	7.18	48.89	0
aqueous solution	-10	1.0696	9.06	49.10	0

182 **2.2 Measurement of the frozen soil hydraulic conductivity**

183 Gardner (1958) proposed that the unsaturated hydraulic conductivity of soil varies with the matric potential

184 as follows:

185 $$K(h) = K_{sat}\exp(\alpha h) \qquad (1)$$

186 where K_{sat} is the saturated hydraulic conductivity, cm/hour, and h is the matric potential or tension, cm H_2O.

187 Wooding (1968) considered that the steady-state unconfined infiltration rate into soil from a circular water

188 source of radius R can be calculated with the following equation:

189 $$Q = \pi R^2 K \left[1 + \frac{4}{\pi R \alpha} \right] \qquad (2)$$

190 where Q is the amount of water entering the soil per unit time, cm^3/h; K is the hydraulic conductivity,

191 cm/hour; and α is a constant. Ankeny et al. (1991) proposed that implementing two successively applied

192 pressure heads h_1 and h_2 could yield the unsaturated hydraulic conductivity, and upon replacing K in Eq. (2)

193 with Eq. (1), the following is obtained:

194 $$Q(h_1) = \pi R^2 K_{sat} \exp(\alpha h_1) \left[1 + \frac{4}{\pi R \alpha} \right] \qquad (3)$$

195 $$Q(h_2) = \pi R^2 K_{sat} \exp(\alpha h_2) \left[1 + \frac{4}{\pi R \alpha} \right] \quad (4)$$

196 Dividing Eq. (4) by Eq. (3) and solving for α yields:

197 $$\alpha = \frac{\ln\left[Q(h_2)/Q(h_1) \right]}{h_2 - h_1} \quad (5)$$

198 where $Q(h_1)$ and $Q(h_2)$ can be measured, h_1 and h_2 are the preset tension values, and α can be calculated with

199 Eq. (5). The result can be substituted into Eq. (3) or (4) to calculate K_{sat}. When the number of tension levels

200 is higher than 2, parameter fitting methods can be applied to improve the accuracy of α and K_{sat} (Hussen and

201 Warrick, 1993).

202 The tension is controlled by the bubble collecting tube of the tension infiltrometer, and different pressure

203 heads h correspond to different pore sizes r. By applying different pressure heads h to the soil surface, water

204 will overcome the surface tension in the corresponding pores and will be discharged, and the infiltration

205 volume is recorded after reaching the stable infiltration state.

206 Under the assumption that the frozen soil pore ice pressure is equal to the atmospheric pressure and that

207 solutes are negligible, the Clausius-Clapeyron equation can be adopted to achieve the interconversion

208 between the soil temperature and suction (Konrad and Morgenstern, 1980;Watanabe et al., 2013), which can

209 be simplified as follows:

210 $$\psi = -L\rho_w \frac{T}{273.15} \quad (6)$$

211 where ψ is the soil suction, kPa; L is the latent heat of fusion of water, 3.34×10^5 J/kg; ρ_w is the density of

212 water, 1 g/cm^3; and T is the subfreezing temperature, °C. After the unit conversion of the soil suction into h

213 (cm H$_2$O), the unsaturated hydraulic conductivity of frozen soil at different negative temperatures can be

214 obtained via substitution into Eq. (2).

215 **2.3 Measurement of the pore size distribution in frozen soil**

216   As a nonuniform medium, soil consists of pores with various pore sizes, and the equation for the soil pore

217   radius r can be obtained from the capillary model (Watson and Luxmoore, 1986):

218    $$r= -\frac{2\sigma \cos \beta}{\rho gh} \qquad (7)$$

219   where σ is the surface tension of the solution, g/s^2; β is the contact angle between the solution and pore wall;

220   ρ is the density of the solution, g/cm^3; g is the acceleration of gravity, m/s^2; and h is the corresponding tension

221   of the tension infiltrometer, cm H_2O.

222   The effective macroporosity θ_m can be calculated for various soil particle sizes based on the Poiseuille

223   equation (Wilson and Luxmoore, 1988):

224    $$\theta_m = 8\mu K_m / \rho gr^2 \qquad (8)$$

225   where μ is the dynamic viscosity of the fluid, $g/(cm*s)$; K_m is the macropore hydraulic conductivity and is

226   defined as the difference between K(h) at various tension gradients, cm/h; and r is the corresponding

227   equivalent pore size. The effective porosity is equal to the number of pores per unit area multiplied by the

228   area of the corresponding pore size. For different pore sizes, the maximum number of effective macropores

229   per unit area N can be calculated with the following equation:

230    $$N=\theta_m / \pi r^2 \qquad (9)$$

231   where N is the number of effective macropores per unit area, and Eq. (7) calculates the minimum value of

232   the pore radius, while the result obtained with Eq. (9) is actually the maximum number of effective

233   macropores per unit area and the maximum porosity.

234   Considering the differences in surface tension and density between the aqueous ethylene glycol solution and

235   water, when calculating the frozen soil pore size distribution, it is necessary to convert the tension into the

236   equivalent pore radius according to Eq. (7), which is classified and subdivided into large and medium pores

237   according to the common classification method (Luxmoore, 1981), the details of which are listed in Table 4,

238 while the corresponding tension values in Table 4 are substituted into the fitting curve equation to calculate

239 the corresponding stable infiltration rate q and unsaturated hydraulic conductivity K.

240 **Table 4**

241 **Tension and equivalent pore radius conversions**

Pore types	Pore radius (mm)	Tension conversion (cm)		
		Water (15℃)	Ethylene glycol aqueous solution (-5℃)	Ethylene glycol aqueous solution (-10℃)
Macroporous	>0.5	0~3	0~1.86	0~1.87
	0.3-0.5	3~5	1.86 ~3.11	1.86 ~3.12
	0.15-0.3	5~10	3.11~6.22	3.12~6.23
Mesoporous	0.1-0.15	10~15	6.22~9.32	6.23~9.35
	0.05-0.1	15~30	9.32~18.65	9.35~18.70

3 Results

242 ### 3.1 Infiltration characteristics of freezing-thawing soils

244 Curves of the recorded cumulative infiltration and infiltration rate were plotted over time, as shown in Figs.

245 3 and 4, respectively. The unfrozen water contents and ice contents of the frozen samples are shown in Table

246 5. The constant α and saturated hydraulic conductivity K_{sat} were calculated under different tensions h and

247 corresponding steady-state infiltration rates q, and the unsaturated hydraulic conductivity under different

248 tensions was calculated with Eq. (1). The stable infiltration rate and unsaturated hydraulic conductivity at

249 different temperatures are shown in Fig. 5, and the details of α and K_{sat} are listed in Table 6.

250 **Table 5**

Unfrozen water contents and ice contents of the frozen samples

Soil types	Unfrozen water contents (cm³/cm³)		Ice contents (cm³/cm³)	
	-5°C	-10°C	-5°C	-10°C
Black soil	0.123	0.101	0.159	0.179
Meadow soil	0.128	0.109	0.145	0.167
Chernozem	0.119	0.097	0.151	0.185
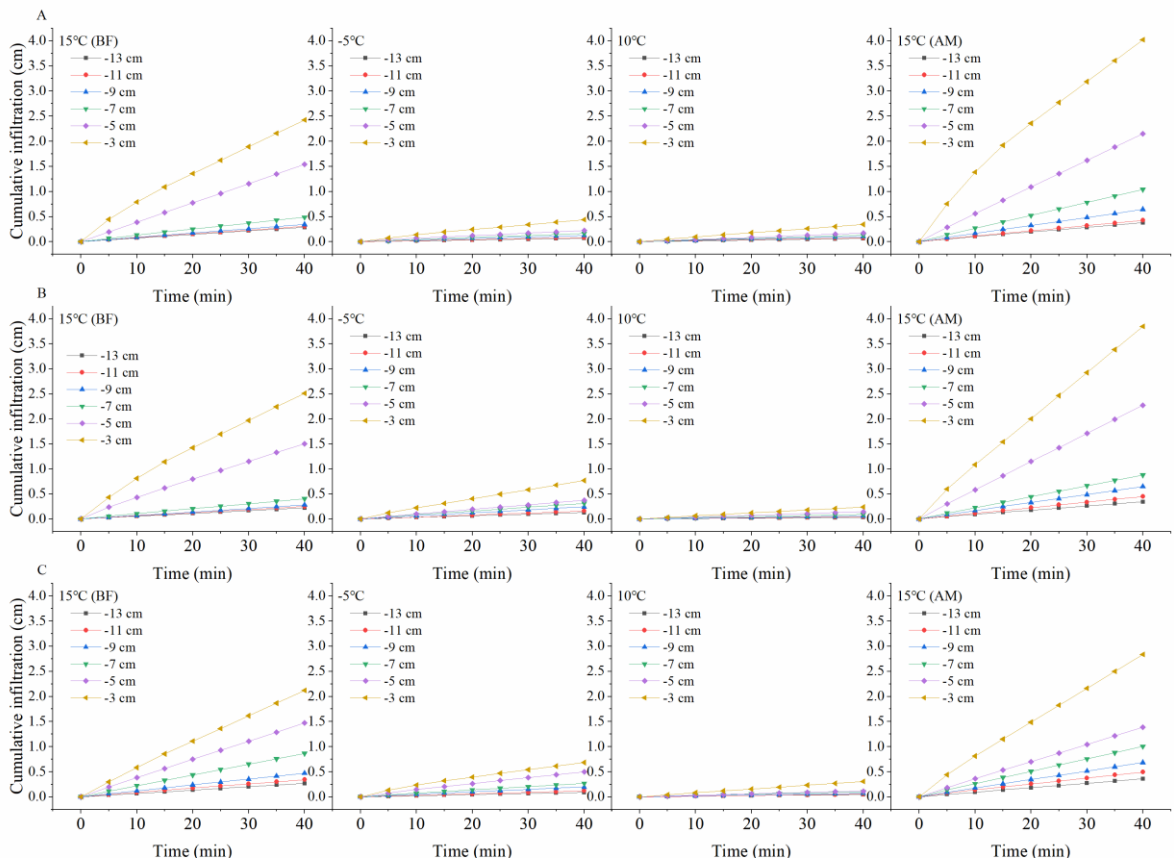
Fig. 3. Cumulative infiltration over time under the different treatments.

Note: A Black Soil; B Meadow Soil; C Chernozem.
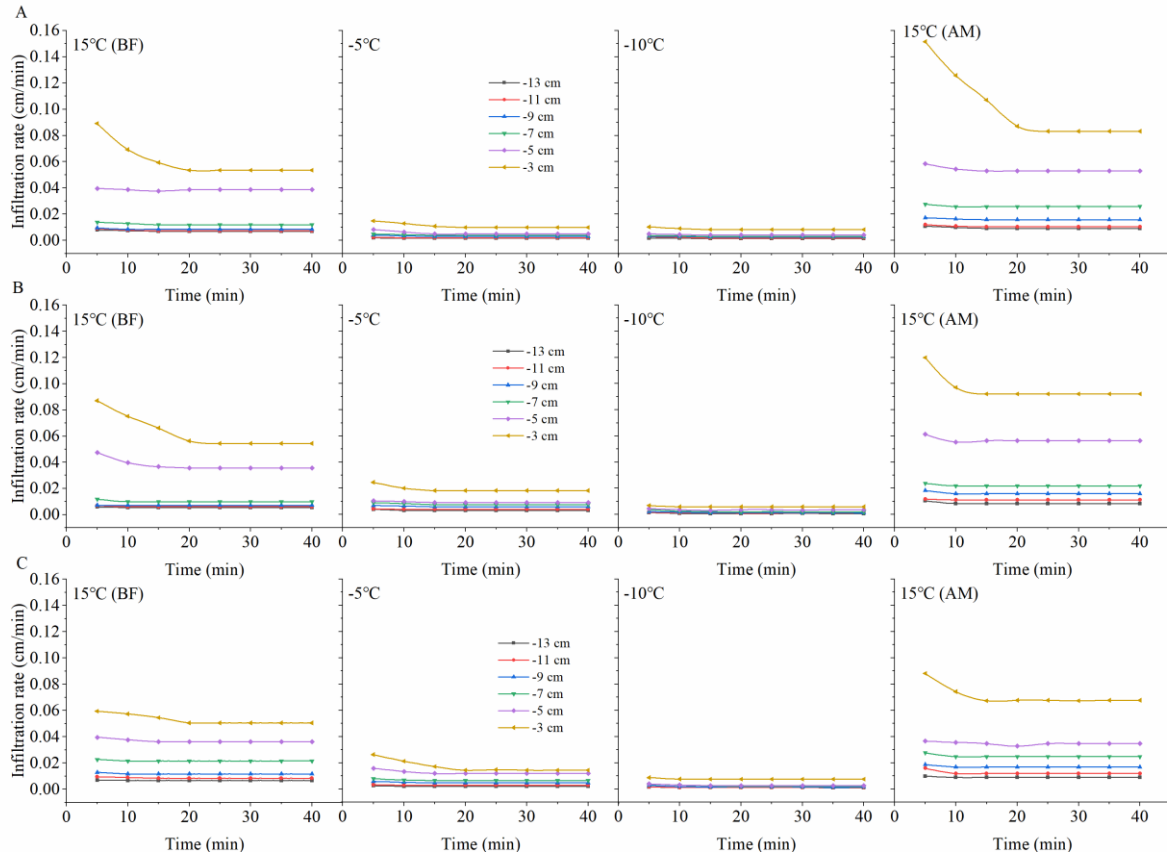
Fig. 4. Infiltration rate over time under the different treatments.

Note: A Black Soil; B Meadow Soil; C Chernozem.

As shown in Figs. 4 and 5, under the different tension conditions, the infiltration capacity of the unfrozen

soil is basically consistent with the findings of field experiments and is highly influenced by the tension

value (Wang et al., 1998). Compared to the room-temperature soil, the cumulative infiltration of frozen soil

slowly increases, and the infiltration rate always remains low, while under the same negative temperature

treatment, the influence of the tension value is also greatly reduced. When the temperature was reduced to -

10°C, few major tension differences were observed except for the maximum tension of -3 cm. Based on the

change in the slope of the two curves, the time for the unfrozen soil to reach the stable infiltration rate usually

ranges from 15~20 min, while the time for the frozen soil to reach the stable infiltration rate is usually 10

min under higher tensions of -3 and -5 cm and 5 min under lower tensions. A comparison of the infiltration

process before and after the freezing and thawing of the soil indicates that overall, the cumulative infiltration

and infiltration rate exhibited varying degrees of increase with increasing tension value, and the increase

amplitude expanded. Moreover, the difference in the cumulative infiltration and infiltration rate between the

low tension levels ranging from -9 to -13 cm after soil thawing was larger than that before soil freezing,

which also indirectly demonstrated that freezing and thawing could further stabilize the soil pore distribution

by affecting the homogeneity, which will be detailed in subsequent sections.

Table 6

Infiltration parameters of the different temperature treatments of the three soil types

Soil types	Temperature (°C)	α (cm/h)	K_{sat} (cm/h)	Permeability (m^2)
Black soil	15 (BF)	0.2742	5.1480	1.66E-09
	-5	0.1993	0.5960	1.14E-09
	-10	0.2028	0.5221	1.25E-09
	15 (AM)	0.2629	7.4658	2.41E-09
Meadow soil	15 (BF)	0.3071	5.9232	1.92E-09
	-5	0.1996	1.1385	2.17E-09
	-10	0.2477	0.4903	1.18E-09
	15 (AM)	0.2934	9.3757	3.03E-09
Chernozem	15 (BF)	0.2166	3.7185	1.20E-09
	-5	0.1907	0.9739	1.86E-09
	-10	0.2508	0.6077	1.46E-09
	15 (AM)	0.2182	5.1283	1.66E-09
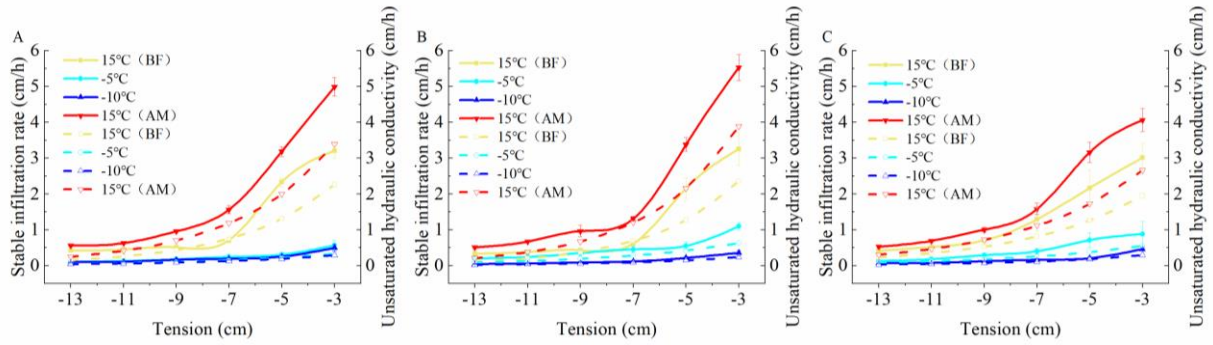
Fig. 5. Variation curves of the unsaturated hydraulic conductivity and stable infiltration rate with the tension for the different treatments of the three soils.

Note: A Black soil; B meadow soil; C chernozem. The solid lines represent the stable infiltration rate, and the dashed lines represent the unsaturated hydraulic conductivity.

By combining Fig. 5 and Table 6, we observe that the three types of soils exhibit a high infiltration capacity under normal temperature conditions. With increasing set tension value, the suction force of the soil matrix gradually weakened, the constraint and maintenance capacity of the matric potential with respect to the soil water decreased, the number of pores involved in the soil water infiltration process increased, and the unsaturated hydraulic conductivity and stable infiltration rate of the three types of soils exhibited different degrees of increase. When the temperature was lowered from 15℃ to -5℃ and remained constant for a certain time, the soil reached the stable frozen state which usually indicated that there were no more drastic changes in temperature and moisture content, the saturated water conductivity of the black soil, meadow soil and chernozem soil decreased by 88.42%, 80.78% and 73.8%, respectively. When the soil temperature was decreased to -10 ℃, due to the presence of liquid water in the pores, the saturated water conductivity still exhibited a certain decrease over the pre-freeze conditions and continued to decrease by 1.43%, 10.94% and 9.85%, respectively. At negative temperatures, the unsaturated hydraulic conductivity decreased considerably and fluctuated within a small range, mainly because the unfrozen water content and saturated hydraulic conductivity were low after soil freezing. Based on a comparing of the -5℃ and -10℃ treatments,

the unsaturated hydraulic conductivity (ANOVA, P=0.72, F=0.14) and stable infiltration rate (ANOVA, P=0.71, F=0.15) of the black soil exhibited almost no significant change, indicating that most of its pores were filled with ice crystals at -5°C and were no longer involved in water infiltration. The unsaturated water conductivity of the meadow and chernozem soils still exhibited a more significant reduction when the freezing temperature was further reduced to -10°C. When the temperature was raised again to 15°C and the soil was completely thawed, the steady infiltration rate and saturated hydraulic conductivity increased with increasing temperature, and the values were higher than those of the soil at the same temperature before freezing. The saturated hydraulic conductivity of the black soil, meadow soil and chernozem increased by 45.02%, 58.63% and 37.91%, respectively, relative to the 15°C (BF) treatment values.

3.2 Pore distribution characteristics of the freezing-thawing soil

Considering the differences in the physical and chemical properties between the infiltration solutions, infiltration parameters such as the hydraulic conductivity and stable infiltration rate alone do not fully reflect the infiltration characteristics and internal pore size of frozen soils. According to Eqs. (7)-(9), the maximum number per unit area N, effective porosity θ_m and percentage of pore flow to saturated flow P corresponding to the different soil pore sizes of the three soils under the different temperature treatments were calculated, as shown in Figs. 6 and 7.

314
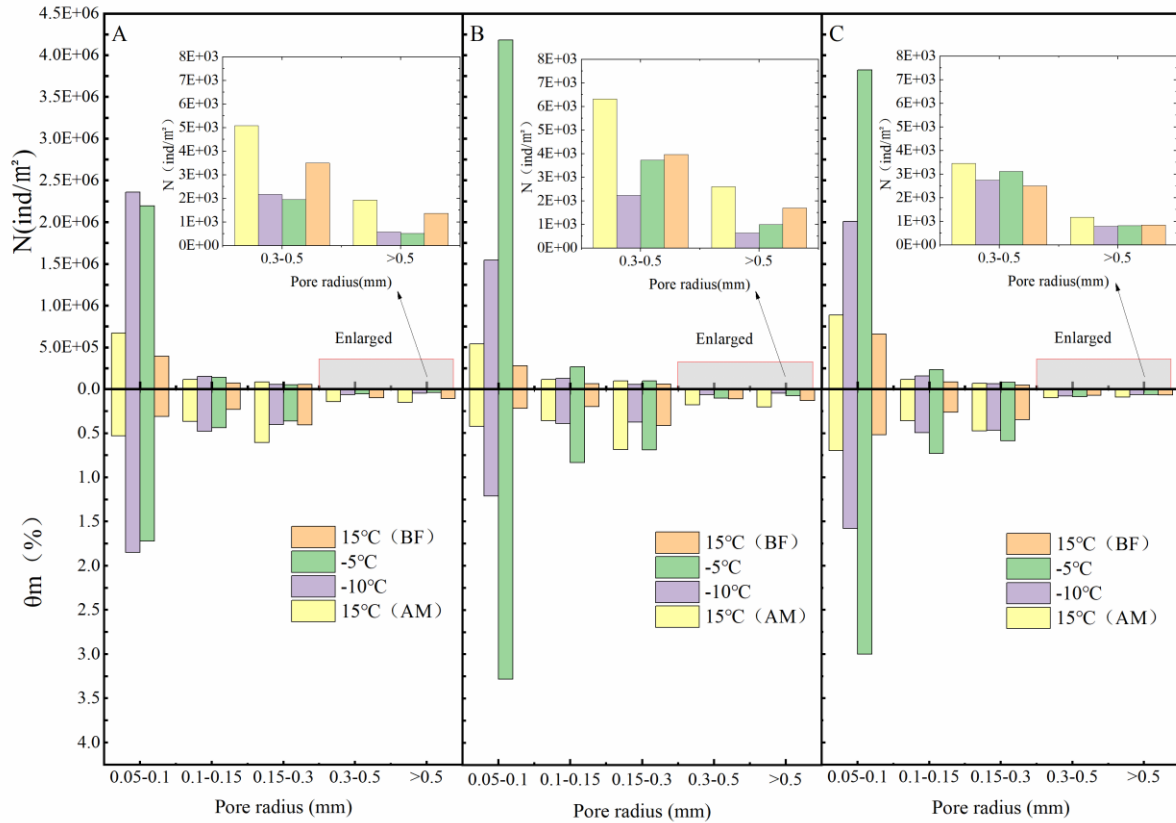
Fig. 6. Number of pores and effective porosity of the different equivalent pores.

316   Note: A Black Soil; B Meadow Soil; C Chernozem.

317
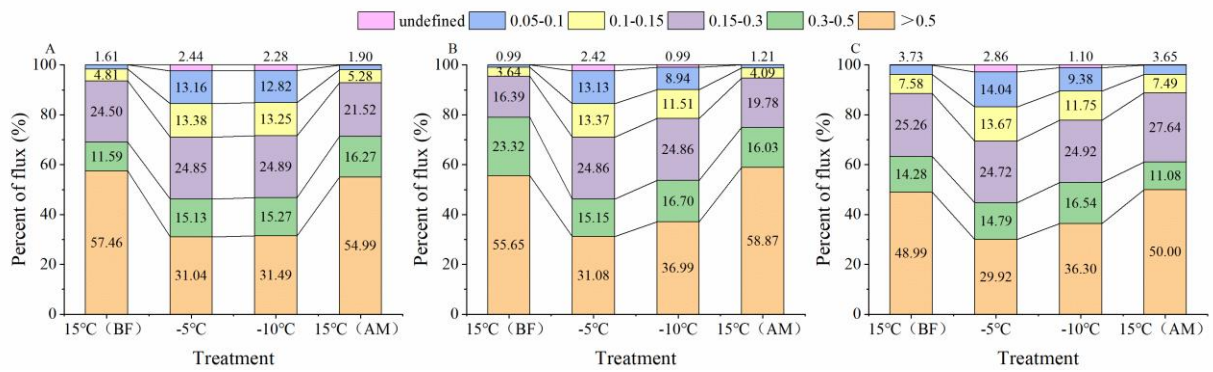
Fig. 7. Percentage of the pore flow in the saturated flow for the different equivalent pore sizes.

319   Note: A Black Soil; B Meadow Soil; C Chernozem.

320   Fig. 6 shows that pores of different equivalent radii widely occur in all three soils, and under all four

321   temperature treatments, the largest N value is that for the medium pores with an equivalent radius of 0.05-

322   0.1 mm, and N gradually decreases with increasing equivalent radius size. Under the two room-temperature

323   treatments at 15°C (BF) and 15°C (AM), the largest number of 0.05- to 0.1-mm medium pores and the

324   smallest number of >0.5-mm macropores differed by two orders of magnitude, and the number of pores of

325   each size exhibited different degrees of increase or decrease in the two treatments at -5°C and -10°C where

326   freezing occurred, with the number of medium pores with an equivalent pore size of 0.05-0.1 mm

327   significantly changing. Increases of more than an order of magnitude were achieved in all three soils, while

328   the macropores with an equivalent pore size of >0.5 mm were generally reduced by an order of magnitude,

329   with the difference in the number of pores of these two sizes reaching four orders of magnitude. This

330   indicates that freezing caused by temperature change significantly alters the soil internal structure, with ice

331   crystals forming in the relatively large pores containing the internal soil moisture, resulting in a large number

332   of smaller pores. Based on an assessment of the two treatments at -5°C and -10°C separately, when the

333   temperature was lowered from -5°C to -10°C, the number of pores in each pore size interval of the meadow

334   and chernozem soils exhibited a significant decrease, while the black soil revealed a small increase, which

335   might be related to the high organic matter content of the black soil. A comparison of the two treatments at

336   15°C (BF) and 15°C (AM) indicated that the number of pores in all three soils increased to different degrees

337   after thawing, and more pores were formed with the melting of ice crystals after the freeze-thaw destruction

338   of the soil particles, which enhanced the soil water conductivity.

339   Comprehensive analysis of Figs. 6 and 7 reveals that before freezing, the θ_m values of the various pore sizes

340   of the black soils, meadow soils and chernozem with an equivalent radius of >0.5 mm were 0.11%, 0.13%

341   and 0.07%, respectively, while the P value reached 57.46%, 55.65% and 48.99%, respectively, with the

342   values of the thawed soil similar to these values. This indicates that for all five soil pore sizes under unfrozen

343   conditions, although the number of macropores with a pore size >0.5 mm was the smallest and the effective

344   porosity was the lowest, their contribution to the saturated flow was usually more than half, and the

345   macropores needed to represent only a small fraction of the pore volume to significantly contribute to the

346   soil water flow. For the frozen soil, the P value of the >0.5-mm macropores was significantly reduced and

347   remained at approximately 30% after the reduction, while the P value of the smaller pore sizes such as 0.15-

348   0.3 mm, 0.1-0.15 mm, and 0.05-0.1 mm, revealed different degrees of increase. Moreover, the smaller the

349   pore size, the greater the P value increased, and the contribution of these pores eventually accounted for

350   more than 10% of the saturated flow. The saturated flow became more evenly distributed across the pores of

351   each size, and the total proportion of medium pores exceeded that of the macropores. This indicates that the

352   freezing action caused obvious changes to the soil structure, pore size and quantity, and although the

353   macropores still played an important role, the infiltration capacity of the frozen soil no longer relied solely

354   on these macropores, and the contribution of certain smaller-sized mesopores to the infiltration capacity of

355   the frozen soil could no longer be neglected. Selecting black soil as an example, the total effective porosity

356   of the pores of each size under the four treatments was 1.15%, 2.62%, 2.84%, and 1.80%, and the P values

357   were 99.97%, 97.56%, 97.72%, and 99.96%, respectively, which implies that the soil water infiltrated almost

358   entirely via the large and medium pores. The small micropores, even in large numbers, contributed little to

359   the infiltration process.

360   **4 Discussion**

361   **4.1 Permeability and hydraulic conductivity of the frozen soil**

362   It is worth noting that the theory underpinning the tension infiltration analysis in this article is based on the

363   assumption that larger pores only flow fully saturated which means no air-water interface inside the pore and

364   excludes the formation of an air-water interface with flowing water in larger pores (Perroux and White, 1988).

365   However, recent work has shown that this flow mode does indeed occur (Beven and Germann, 2013;Nimmo,

366   2012, 2010). In addition, in unfrozen tension infiltrometer experiments, the soil moisture is assumed to be

367   that imposed by the applied tension, whereas in the experiments with frozen samples, the applied tension is

368   assumed to affect only the pores that are active during infiltration.

369   In the field environment, although it is difficult to accurately measure the infiltration rate of frozen soils

370   using traditional instruments and methods such as single-loop infiltrators, the obtained test results still

371   demonstrate that the infiltration capacity decreases by one or more orders of magnitude when the soil is

372   frozen (Stähli et al., 2004). Although the cumulative infiltration and infiltration rate of frozen soil are low,

373   the presence of unfrozen water allows a certain amount of infiltration flow to be maintained in the soil. When

374   water is applied as the infiltration solution, the low temperature of the frozen soil easily causes the infiltration

375   water to freeze, thus forming a thin layer of ice on the soil particle surface and delaying the subsequent

376   infiltration of water. This phenomenon results in a low infiltration rate after the freezing of soils with a high

377   initial water content and a relatively high infiltration rate after the freezing of dry soils (Watanabe et al.,

378   2013), because the higher the ice content is, the more latent heat needs to be overcome to melt any ice crystals,

379   resulting in a weakened propagation of the melting front, thus limiting the infiltration rate so that it is

380   controlled by the downward movement of the melting leading edge of the ice crystals (Pittman et al., 2020).

381   During the measurements using the tension infiltrator in this study, the sensor temperature always remained

382   consistent with the soil temperature, indicating that the use of an aqueous glycol solution could be a useful

383   way to avoid the problem of freezing of the infiltration solution. In addition, the hydraulic conductivity of

384   frozen soils with different capacities and at various water flow rates was demonstrated not to greatly differ

385   (Watanabe and Osada, 2017).

386   Whether water or other low-freezing point solutions are applied as infiltration media, the hydraulic

387   conductivity of frozen soil significantly changes only within a limited temperature range above -0.5°C

388   depending on the unfrozen water and ice contents, and at a soil temperature below -0.5°C, the hydraulic

389   conductivity usually decreases to less than 10^{-10} m/s (Watanabe and Osada, 2017;Williams and Burt, 1974).

390   The unsaturated hydraulic conductivity in our experiments was measured at a set tension level, and according

391   to Eq. (6), the soil substrate potential increases by 125 m for every 1°C decrease in temperature (Williams

392   and Smith, 1989), while the frozen soil hydraulic conductivity calculated at -5°C and -10°C, which

393   corresponds to the actual matric potential, is much lower than 10^{-10} m/s, close to the zero point of the

394   unsaturated hydraulic conductivity variation curves in Fig. 5, and can be ignored. This suggests that even

395   under ideal conditions where no heat exchange occurs between the infiltration solution and the soil and no

396   freezing of the infiltration water takes place to prevent subsequent infiltration, the unsaturated hydraulic

397   conductivity of frozen soil is so low that the frozen soil at lower temperatures in its natural state could be

398   considered impermeable, with respect to both water and other solutions. It should also be noted that we used

399   different liquids at different temperatures and that the difference in infiltration parameters such as K_{sat} with

400   temperature is related to the different viscosities of the liquid. It is predictable that if water is also used in

401   frozen soils, such differences will be relatively insignificant as the ice melts.

402   **4.2 Effect of freeze-thaw cycles on soil pore distribution**

403   In our study, the N value after freezing for the different types of soil was approximately 1000-2000/m^2 base

404   on the tension infiltrator, which agreed well with other studies such as conventional soil ring methods

405   (Pittman et al., 2020) or geophysical imaging techniques such as X-ray and CT (Ding et al., 2019;Holten et

406   al., 2018) and remained at the same magnitude, indicating that the method is generally reliable. Compared

407   with saturated frozen soils (Ding et al., 2019), the effect of freeze-thaw cycles on the pore distribution of

408   unsaturated frozen soil is also significant. Moreover, it should be noted that instruments such as CT are

409   usually expensive and difficult to carry, tension infiltrators are affordable and widely used, and combined

410   with temperature control equipment, they will be helpful for field measurements of macroporosity in frozen

411   soils. The freeze-thaw effect significantly improves the water conductivity of the different types of soils

412   because it increases the porosity, decreases the soil compactness and dry weight, and thus increases the soil

413   water conductivity (Fouli et al., 2013). On this basis, we also found that the freeze/thaw process significantly

414   altered the size and number of soil pores, especially after freezing, and the number of macropores decreased,

415   while the contribution of macropores to the saturated flow decreased. The proportion of the saturated flow

416   in the mesopores with a pore size of <0.3 mm approached or even exceeded the proportion in the macropores,

417   indicating that the soil water inside relatively large pores is more likely to freeze, which in turn creates a

418   large number of small pores, whereas the water transfer process in unfrozen soils primarily relies on the

419   macropores, with obvious differences (Wilson and Luxmoore, 1988;Watson and Luxmoore, 1986). The

420   unsaturated water conductivity of the frozen soils measured in this study was quite low, but under human

421   control (Watanabe and Kugisaki, 2017) or natural conditions in the field (Espeby, 1990), water has been

422   shown to infiltrate frozen soils through macropores as long as the pore size is large enough. Considering that

423   the soil in this experiment was disturbed soil that had been air dried and sieved, although the macropores

424   created by tillage practices (Lipiec et al., 2006) and invertebrate activities (Lavelle et al., 2006) were

425   excluded, due to the inherent heterogeneity of the soil particles, macropores remain in the uniformly filled

426   soil column (Cortis and Berkowitz, 2004;Oswald et al., 1997), and these macropores still played a role in

427   determining the infiltration water flow. In addition, according to the equations of N and θ_m, it can be found

428   that the main source of their uncertainty is the value of the pore radius r, and Eq. (7) calculates the minimum

429   value of pore radius, while the result obtained with Eq. (9) is in fact the upper limit of effective macropores

430   per unit area and effective porosity, which may also lead to a certain overestimation. Furthermore, freezing

431   of water may also have a potential effect on the microstructure of soil pores(Wan and Yang, 2020).

432   There are still only a few studies related to frozen soil macropore flow and pore distribution; consequently,

more data should be acquired, and more models should be developed to better understand water movement in frozen soil regions. The experiments in this paper are based on repacked soils that were subjected to the first freeze-thaw cycle in the laboratory, and the conclusions may not be comprehensive. In subsequent studies, we will consider applying the methods used in this paper to field experiments to examine the dynamics of the infiltration capacity and pore distribution in nonhomogeneous soils during whole freeze-thaw periods under real outdoor climatic conditions, such as lower temperatures and more severe freeze-thaw cycles, but the infiltration solution must be carefully selected; as ethylene glycol has low toxicity, to prevent contamination of agricultural soils and crops, a certain concentration of lactose could be considered (Burt and Williams, 1976;Williams and Burt, 1974). At room temperature, an ethylene glycol aqueous solution and water have similar densities and relatively similar viscosities. We have compared these two infiltration solutions in unfrozen soil field experiments, and the infiltration and pore conditions were basically similar, so we still used an aqueous glycol solution in the frozen soil laboratory experiment. Measurements should focus on frozen soil layers at different depths, especially in the vicinity of freezing peaks, and the spatial variability in the distribution of frozen soil pores should be investigated. This work helps to improve the accuracy of simulations such as those of frozen soil water and heat movement or snowmelt water infiltration processes.

5 Conclusions

In this paper, the infiltration capacity of soil columns under four temperature treatments representing various freeze-thaw stages was measured, and the distribution of the pores of various sizes within the soil was calculated based on the measurements by applying an aqueous ethylene glycol solution with a tension infiltrator in the laboratory. The results revealed that for the three types of soils, i.e., black soil, meadow soil and chernozem, the macropores, which accounted for only approximately 0.1% to 0.2% of the soil volume

455 at room temperature, contributed approximately 50% to the saturated flow, and after freezing, the proportion

456 of macropores decreased to 0.05% to 0.1%, while their share of the saturated flow decreased to

457 approximately 30%. Coupled with the even smaller mesopores, the large and medium pores, accounting for

458 approximately 1% to 2% of the soil volume, conducted almost all of the soil moisture under saturated

459 conditions. Freezing decreased the number of macropores and increased the number of smaller-sized

460 mesopores, thereby significantly increasing their contribution to the frozen soil infiltration capacity so that

461 the latter was no longer solely dependent on the macropores. The infiltration parameters and pore distribution

462 of the black soil were the least affected by the different negative freezing temperatures under the same

463 moisture content and weight capacity conditions, while those of the meadow soil were the most impacted.

Data availability

465 Data used in this study are available at Figshare (doi: 10.6084/m9.figshare.12965123).

Author contributions

467 Ruiqi Jiang designed the research program. Tianxiao Li and Ruiqi Jiang built and deployed the soil column

468 and instruments with assistance from Qinglin Li and Renjie Hou. Dong Liu and Qiang Fu provided funding

469 for test equipment. Song Cui collected soil samples in the field. Ruiqi Jiang and Tianxiao Li analyzed the

470 laboratory data. Ruiqi Jiang prepared the manuscript with comments from Tianxiao Li and Dong Liu.

Competing interests

472 The authors declare that they have no conflicts of interest

Acknowledgements

474 We acknowledge that this research was supported by the National Natural Science Foundation of China

475 (51679039), the National Science Fund for Distinguished Young Scholars (51825901), the Heilongjiang

476 Provincial Science Fund for Distinguished Young Scholars (YQ2020E002),"Young Talents" Project of

477   Northeast Agricultural University(18QC28), and the China Postdoctoral Science Foundation Grant

478   (2019M651247).

References

480   Andersland, O. B., Wiggert, D. C., and Davies, S. H.: Hydraulic conductivity of frozen granular soils, J
481 Environ Eng, 122, 212-216, 10.1061/(ASCE)0733-9372(1996)122:3(212), 1996.

482   Angulo-Jaramillo, R., Vandervaere, J.-P., Roulier, S., Thony, J.-L., Gaudet, J.-P., and Vauclin, M.: Field
483 measurement of soil surface hydraulic properties by disc and ring infiltrometers: A review and recent
484 developments, Soil and Tillage Research, 55, 1-29, 10.1016/S0167-1987(00)00098-2, 2000.

485   Ankeny, M. D., Ahmed, M., Kaspar, T. C., and Horton, R.: Simple field method for determining
486 unsaturated hydraulic conductivity, Soil Sci Soc Am J, 55, 467-470,
487 10.2136/sssaj1991.03615995005500020028x, 1991.

488   Azmatch, T. F., Sego, D. C., Arenson, L. U., and Biggar, K. W.: Using soil freezing characteristic curve to
489 estimate the hydraulic conductivity function of partially frozen soils, Cold Reg. Sci. Technol, 83, 103-109,
490 10.1016/j.coldregions.2012.07.002, 2012.

491   Beven, K., and Germann, P.: Macropores and water flow in soils revisited, Water Resour Res, 49, 3071-
492 3092, 10.1002/wrcr.20156, 2013.

493   Bodhinayake, W., Si, B. C., and Xiao, C.: New method for determining water‐conducting macro‐and
494 mesoporosity from tension infiltrometer, Soil Sci Soc Am J, 68, 760-769, 10.2136/sssaj2004.0760, 2004.

495   Bureau, H. L. A.: Heilongjiang soil, Agriculture Press, Beijing, 1992.

496   Burt, T., and Williams, P. J.: Hydraulic conductivity in frozen soils, Earth Surface Processes, 1, 349-360,
497 10.1002/esp.3290010404, 1976.

498   Campbell, G. S.: Soil physics with BASIC: transport models for soil-plant systems, Elsevier, Amsterdam,
499 1985.

500   Cheng, Q., Xu, Q., Cheng, X., Yu, S., Wang, Z., Sun, Y., Yan, X., and Jones, S. B.: In-situ estimation of
501 unsaturated hydraulic conductivity in freezing soil using improved field data and inverse numerical modeling,
502 Agr Forest Meteorol, 279, 107746, 10.1016/j.agrformet.2019.107746, 2019.

503   Cortis, A., and Berkowitz, B.: Anomalous transport in "classical" soil and sand columns, Soil Sci Soc Am
504 J, 68, 1539-1548, 10.2136/sssaj2004.1539, 2004.

505   Daniel, Stadler, and, Hannes, Flühler, and, Per-Erik, and Jansson: Modelling vertical and lateral water flow
506 in frozen and sloped forest soil plots, Cold Regions Science & Technology, 10.1016/S0165-232X(97)00017-7,
507 1997.

508   Demand, D., Selker, J. S., and Weiler, M.: Influences of macropores on infiltration into seasonally frozen
509 soil, Vadose Zone J, 18, 1-14, 10.2136/vzj2018.08.0147, 2019.

510   Ding, B., Rezanezhad, F., Gharedaghloo, B., Cappellen, P. V., and Passeport, E.: Bioretention cells under
511 cold climate conditions: Effects of freezing and thawing on water infiltration, soil structure, and nutrient
512 removal, Sci Total Environ, 649, 2019.

513   Espeby, B.: Tracing the origin of natural waters in a glacial till slope during snowmelt, J Hydrol, 118, 107-
514 127, 10.1016/0022-1694(90)90253-T, 1990.

515   Flerchinger, G. N., and Saxton, K. E.: Simultaneous Heat and Water Model of a Freezing Snow-Residue-
516 Soil System I. Theory and Development, American Society of Agricultural Engineers, 10.13031/2013.31041,
517 1989.

Fouli, Y., Cade-Menun, B. J., and Cutforth, H. W.: Freeze–thaw cycles and soil water content effects on infiltration rate of three Saskatchewan soils, Can J Soil Sci, 93, 485-496, 10.4141/CJSS2012-060, 2013.

Fu, Q., Zhao, H., Li, T., Hou, R., Liu, D., Ji, Y., Zhou, Z., and Yang, L.: Effects of biochar addition on soil hydraulic properties before and after freezing-thawing, Catena, 176, 112-124, 10.1016/j.catena.2019.01.008, 2019.

Gao, B., Yang, D., Qin, Y., Wang, Y., Li, H., Zhang, Y., and Zhang, T.: Change in frozen soils and its effect on regional hydrology, upper Heihe basin, northeastern Qinghai-Tibetan Plateau, Cryosphere, 12, 657-673, 2018.

Gao, H., and Shao, M.: Effects of temperature changes on soil hydraulic properties, Soil Till Res, 153, 10.1016/j.still.2015.05.003, 2015.

Gardner, W.: Some steady-state solutions of the unsaturated moisture flow equation with application to evaporation from a water table, Soil Sci, 85, 228-232, 10.1097/00010694-195804000-00006, 1958.

Granger, R. J., Gray, D. M., and Dyck, G. E.: Snowmelt infiltration to frozen Prairie soils, Can J Earth Sci, 21, 669-677, 10.1139/e84-073, 1984.

Grevers, M., JONG, E. D., and St. Arnaud, R.: The characterization of soil macroporosity with CT scanning, Can J Soil Sci, 69, 629-637, 10.4141/cjss89-062, 1989.

Harlan, R.: Analysis of coupled heat‐fluid transport in partially frozen soil, Water Resour Res, 9, 1314-1323, 10.1029/WR009i005p01314, 1973.

Hayashi, M., Kamp, G. V. D., and Schmidt, R.: Focused infiltration of snowmelt water in partially frozen soil under small depressions, J Hydrol, 270, 214-229, 10.1016/S0022-1694(02)00287-1, 2003.

Hayashi, M.: The Cold Vadose Zone: Hydrological and Ecological Significance of Frozen-Soil Processes, Vadose Zone J, 12, 10.2136/vzj2013.03.0064, 2013.

Holten, R., Be, F. N., Almvik, M., Katuwal, S., and Eklo, O. M.: The effect of freezing and thawing on water flow and MCPA leaching in partially frozen soil, J Contam Hydrol, 219, 72-85, 2018.

Hussen, A., and Warrick, A.: Alternative analyses of hydraulic data from disc tension infiltrometers, Water Resour Res, 29, 4103-4108, 10.1029/93WR02404, 1993.

Jame, Y. W., and Norum, D. I.: Heat and mass transfer in a freezing unsaturated porous medium, Water Resour Res, 16, 811–819, 1980.

Jarvis, N.: A review of non‐equilibrium water flow and solute transport in soil macropores: Principles, controlling factors and consequences for water quality, Eur J Soil Sci, 58, 523-546, 10.1111/j.1365-2389.2007.00915.x, 2007.

Jarvis, N., Koestel, J., and Larsbo, M.: Understanding Preferential Flow in the Vadose Zone: Recent Advances and Future Prospects, Vadose Zone J, 15, 10.2136/vzj2016.09.0075, 2016.

Kamp, G. v. d., Hayashi, M., and Gallén, D.: Comparing the hydrology of grassed and cultivated catchments in the semi-arid Canadian prairies, Hydrol Process, 10.1002/hyp.1157, 2003.

Konrad, J.-M., and Morgenstern, N. R.: A mechanistic theory of ice lens formation in fine-grained soils, Can Geotech J, 17, 473-486, 10.1139/t80-056, 1980.

Lavelle, P., Decaëns, T., Aubert, M., Barot, S. b., Blouin, M., Bureau, F., Margerie, P., Mora, P., and Rossi, J.-P.: Soil invertebrates and ecosystem services, Eur J Soil Biol, 42, S3-S15, 10.1016/j.ejsobi.2006.10.002, 2006.

Lewis, J., and Sjöstrom, J.: Optimizing the experimental design of soil columns in saturated and unsaturated transport experiments, J Contam Hydrol, 115, 1-13, 2010.

Lipiec, J., Kuś, J., Słowińska-Jurkiewicz, A., and Nosalewicz, A.: Soil porosity and water infiltration as influenced by tillage methods, Soil and Tillage research, 89, 210-220, 10.1016/j.still.2005.07.012, 2006.

Lu, N., and Likos, W. J.: Unsaturated soil mechanics, Wiley, Hoboken, 2004.

Lundin, L.-C.: Hydraulic properties in an operational model of frozen soil, J Hydrol, 118, 289-310, 10.1016/0022-1694(90)90264-X, 1990.

Luxmoore, R.: Micro-, meso-, and macroporosity of soil, Soil Sci Soc Am J, 45, 671-672, 10.2136/sssaj1981.03615995004500030051x, 1981.

McCauley, C. A., White, D. M., Lilly, M. R., and Nyman, D. M.: A comparison of hydraulic conductivities, permeabilities and infiltration rates in frozen and unfrozen soils, Cold Reg. Sci. Technol, 34, 117-125, 10.1016/S0165-232X(01)00064-7, 2002.

Mohammed, A. A., Kurylyk, B. L., Cey, E. E., and Hayashi, M.: Snowmelt infiltration and macropore flow in frozen soils: Overview, knowledge gaps, and a conceptual framework, Vadose Zone J, 17, 1-15, 10.2136/vzj2018.04.0084, 2018.

Mohammed, A. A., Pavlovskii, I., Cey, E. E., and Hayashi, M.: Effects of preferential flow on snowmelt partitioning and groundwater recharge in frozen soils, Hydrol Earth Syst Sc, 23, 5017-5031, 10.5194/hess-23-5017-2019, 2019.

Nimmo, J. R.: Theory for Source-Responsive and Free-Surface Film Modeling of Unsaturated Flow, Vadose Zone J, 9, 295-306, 10.2136/vzj2009.0085, 2010.

Nimmo, J. R.: Preferential flow occurs in unsaturated conditions, Hydrol Process, 26, 786-789, 10.1002/hyp.8380, 2012.

Nixon, J.: Discrete ice lens theory for frost heave in soils, Can Geotech J, 28, 843-859, 10.1139/t91-102, 1991.

Oswald, S., Kinzelbach, W., Greiner, A., and Brix, G.: Observation of flow and transport processes in artificial porous media via magnetic resonance imaging in three dimensions, Geoderma, 80, 417-429, 10.1016/S0016-7061(97)00064-5, 1997.

Oztas, T., and Fayetorbay, F.: Effect of freezing and thawing processes on soil aggregate stability, Catena, 52, 1-8, 10.1016/S0341-8162(02)00177-7, 2003.

Peng, X., Frauenfeld, O. W., Cao, B., Wang, K., Wang, H., Su, H., Huang, Z., Yue, D., and Zhang, T.: Response of changes in seasonal soil freeze/thaw state to climate change from 1950 to 2010 across china, Journal of Geophysical Research Earth Surface, 10.1002/2016JF003876, 2016.

Perroux, K. M., and White, I.: Designs for Disc Permeameters, Soil Sci Soc Am J, 52, 1205-1215, 10.2136/sssaj1988.03615995005200050001x, 1988.

Pittman, F., Mohammed, A., and Cey, E.: Effects of antecedent moisture and macroporosity on infiltration and water flow in frozen soil, Hydrol Process, 34, 795-809, 10.1002/hyp.13629, 2020.

Smith, M.: Observations of soil freezing and frost heave at Inuvik, Northwest Territories, Canada, Can J Earth Sci, 22, 283-290, 10.1016/0148-9062(85)90073-7, 1985.

Spaans, E. J.: The soil freezing characteristic: Its measurement and similarity to the soil moisture characteristic, 1994.

Spaans, E. J., and Baker, J. M.: The soil freezing characteristic: Its measurement and similarity to the soil moisture characteristic, Soil Sci Soc Am J, 60, 13-19, 10.2136/sssaj1996.03615995006000010005x, 1996.

Stadler, D., Sta¨hli, M., Aeby, P., and Flu¨hler, H.: Dye tracing and image analysis for quantifying water infiltration into frozen soils, Soil Sci Soc Am J, 64, 505-516, 10.2136/sssaj2000.642505x, 2000.

Stähli, M., Bayard, D., Wydler, H., and Flühler, H.: Snowmelt Infiltration into Alpine Soils Visualized by Dye Tracer Technique, Arctic Antarctic & Alpine Research, 36, 128-135, 10.1657/1523-0430(2004)036[0128:SIIASV]2.0.CO;2, 2004.

Taina, I. A., Heck, R. J., Deen, W., and Ma, E. Y.: Quantification of freeze–thaw related structure in cultivated topsoils using X-ray computer tomography, Can J Soil Sci, 93, 533-553, 10.4141/CJSS2012-044,

2013.

Tarnawski, V. R., and Wagner, B.: On the prediction of hydraulic conductivity of frozen soils, Can Geotech J, 33, 176-180, 10.1139/t96-033, 1996.

Wan, X., and Yang, Z. J.: Pore water freezing characteristic in saline soils based on pore size distribution, Cold Reg. Sci. Technol, 173, 103030.103031-103030.103012, 2020.

Wang, D., Yates, S., and Ernst, F.: Determining soil hydraulic properties using tension infiltrometers, time domain reflectometry, and tensiometers, Soil Sci Soc Am J, 62, 318-325, 10.2136/sssaj1998.03615995006200020004x 1998.

Wang, X., Chen, R., Liu, G., Yang, Y., Song, Y., Liu, J., Liu, Z., Han, C., Liu, X., Guo, S., Wang, L., and Zheng, Q.: Spatial distributions and temporal variations of the near-surface soil freeze state across China under climate change, Global Planet Change, 172, 150-158, 10.1016/j.gloplacha.2018.09.016, 2019.

Watanabe, K., and Flury, M.: Capillary bundle model of hydraulic conductivity for frozen soil, Water Resour Res, 44, 10.1029/2008WR007012, 2008.

Watanabe, K., and Wake, T.: Hydraulic conductivity in frozen unsaturated soil, Proceedings of the 9th International Conference on Permafrost, 2008, 1927-1932,

Watanabe, K., Kito, T., Dun, S., Wu, J. Q., Greer, R. C., and Flury, M.: Water infiltration into a frozen soil with simultaneous melting of the frozen layer, Vadose Zone J, 12, vzj2011.0188, 10.2136/vzj2011.0188, 2013.

Watanabe, K., and Kugisaki, Y.: Effect of macropores on soil freezing and thawing with infiltration, Hydrol Process, 31, 270-278, 10.1002/hyp.10939, 2017.

Watanabe, K., and Osada, Y.: Simultaneous measurement of unfrozen water content and hydraulic conductivity of partially frozen soil near 0 C, Cold Reg. Sci. Technol, 142, 79-84, 10.1016/j.coldregions.2017.08.002, 2017.

Watson, K., and Luxmoore, R.: Estimating macroporosity in a forest watershed by use of a tension infiltrometer, Soil Sci Soc Am J, 50, 578-582, 10.2136/sssaj1986.03615995005000030007x, 1986.

Williams, P., and Burt, T.: Measurement of hydraulic conductivity of frozen soils, Can Geotech J, 11, 647-650, 10.1139/t74-066, 1974.

Williams, P. J., and Smith, M. W.: The frozen earth: fundamentals of geocryology, Cambridge University Press, 1989.

Wilson, G., and Luxmoore, R.: Infiltration, macroporosity, and mesoporosity distributions on two forested watersheds, Soil Sci Soc Am J, 52, 329-335, 10.2136/sssaj1988.03615995005200020005x, 1988.

Wooding, R.: Steady infiltration from a shallow circular pond, Water Resour Res, 4, 1259-1273, 10.1029/WR004i006p01259, 1968.

Zhao, Y., Nishimura, T., Hill, R., and Miyazaki, T.: Determining hydraulic conductivity for air‐filled porosity in an unsaturated frozen soil by the multistep outflow method, Vadose Zone J, 12, 1-10, 10.2136/vzj2012.0061, 2013.